

Search for New Dielectron Resonances and Randall-Sundrum Gravitons at the Collider Detector at Fermilab

T. Aaltonen,²¹ B. Álvarez González,^{9,x} S. Amerio,^{41a} D. Amidei,³² A. Anastassov,³⁶ A. Annovi,¹⁷ J. Antos,¹² G. Apollinari,¹⁵ J. A. Appel,¹⁵ A. Apresyan,⁴⁶ T. Arisawa,⁵⁶ A. Artikov,¹³ J. Asaadi,⁵¹ W. Ashmanskas,¹⁵ B. Auerbach,⁵⁹ A. Aurisano,⁵¹ F. Azfar,⁴⁰ W. Badgett,¹⁵ A. Barbaro-Galtieri,²⁶ V. E. Barnes,⁴⁶ B. A. Barnett,²³ P. Barria,^{44c,44a} P. Bartos,¹² M. Baucé,^{41b,41a} G. Bauer,³⁰ F. Bedeschi,^{44a} D. Beecher,²⁸ S. Behari,²³ G. Bellettini,^{44b,44a} J. Bellinger,⁵⁸ D. Benjamin,¹⁴ A. Beretvas,¹⁵ A. Bhatti,⁴⁸ M. Binkley,^{15,a} D. Bisello,^{41b,41a} I. Bizjak,^{28,bb} K. R. Bland,⁶ B. Blumenfeld,²³ A. Bocci,¹⁴ A. Bodek,⁴⁷ D. Bortoletto,⁴⁶ J. Boudreau,⁴⁵ A. Boveia,¹¹ B. Brau,^{15,b} L. Brigliadori,^{6b,6a} A. Brisuda,¹² C. Bromberg,³³ E. Brucken,²¹ M. Bucciantonio,^{44b,44a} J. Budagov,¹³ H. S. Budd,⁴⁷ S. Budd,²² K. Burkett,¹⁵ G. Busetto,^{41b,41a} P. Bussey,¹⁹ A. Buzatu,³¹ C. Calancha,²⁹ S. Camarda,⁴ M. Campanelli,³³ M. Campbell,³² F. Canelli,^{11,15} A. Canepa,⁴³ B. Carls,²² D. Carlsmith,⁵⁸ R. Carosi,^{44a} S. Carrillo,^{16,l} S. Carron,¹⁵ B. Casal,⁹ M. Casarsa,¹⁵ A. Castro,^{6b,6a} P. Catastini,¹⁵ D. Cauz,^{52a} V. Cavaliere,^{44b,44a} M. Cavalli-Sforza,⁴ A. Cerri,^{26,g} L. Cerrito,^{28,r} Y. C. Chen,¹ M. Chertok,⁷ G. Chiarelli,^{44a} G. Chlachidze,¹⁵ F. Chlebana,¹⁵ K. Cho,²⁵ D. Chokheli,¹³ J. P. Chou,²⁰ W. H. Chung,⁵⁸ Y. S. Chung,⁴⁷ C. I. Ciobanu,⁴² M. A. Ciocci,^{44c} A. Clark,¹⁸ G. Compostella,^{41b,41a} M. E. Convery,¹⁵ J. Conway,⁷ M. Corbo,⁴² M. Cordelli,¹⁷ C. A. Cox,⁷ D. J. Cox,⁷ F. Crescioli,^{44b,44a} C. Cuenca Almenar,⁵⁹ J. Cuevas,^{9,x} R. Culbertson,¹⁵ D. Dagenhart,¹⁵ N. d'Ascenzo,^{42,v} M. Datta,¹⁵ P. de Barbaro,⁴⁷ S. De Cecco,^{49a} G. De Lorenzo,⁴ M. Dell'Orso,^{44b,44a} C. Deluca,⁴ L. Demortier,⁴⁸ J. Deng,^{14,d} M. Deninno,^{6a} F. Devoto,²¹ M. d'Errico,^{41b,41a} A. Di Canto,^{44b,44a} B. Di Ruzza,^{44a} J. R. Dittmann,⁶ M. D'Onofrio,²⁷ S. Donati,^{44b,44a} P. Dong,¹⁵ M. Dorigo,^{52a} T. Dorigo,^{41a} K. Ebina,⁵⁶ A. Elagin,⁵¹ A. Eppig,³² R. Erbacher,⁷ D. Errede,²² S. Errede,²² N. Ershaidat,^{42,aa} R. Eusebi,⁵¹ H. C. Fang,²⁶ S. Farrington,⁴⁰ M. Feindt,²⁴ J. P. Fernandez,²⁹ C. Ferrazza,^{44d,44a} R. Field,¹⁶ G. Flanagan,^{46,t} R. Forrest,⁷ M. J. Frank,⁶ M. Franklin,²⁰ J. C. Freeman,¹⁵ Y. Funakoshi,⁵⁶ I. Furic,¹⁶ M. Gallinaro,⁴⁸ J. Galyardt,¹⁰ J. E. Garcia,¹⁸ A. F. Garfinkel,⁴⁶ P. Garosi,^{44c,44a} H. Gerberich,²² E. Gerchtein,¹⁵ S. Giagu,^{49b,49a} V. Giakoumopoulou,³ P. Giannetti,^{44a} K. Gibson,⁴⁵ C. M. Ginsburg,¹⁵ N. Giokaris,³ P. Giromini,¹⁷ M. Giunta,^{44a} G. Giurgiu,²³ V. Glagolev,¹³ D. Glenzinski,¹⁵ M. Gold,³⁵ D. Goldin,⁵¹ N. Goldschmidt,¹⁶ A. Golossanov,¹⁵ G. Gomez,⁹ G. Gomez-Ceballos,³⁰ M. Goncharov,³⁰ O. González,²⁹ I. Gorelov,³⁵ A. T. Goshaw,¹⁴ K. Goulianos,⁴⁸ S. Grinstein,⁴ C. Grosso-Pilcher,¹¹ R. C. Group,^{55,15} J. Guimaraes da Costa,²⁰ Z. Gunay-Unalan,³³ C. Haber,²⁶ S. R. Hahn,¹⁵ E. Halkiadakis,⁵⁰ A. Hamaguchi,³⁹ J. Y. Han,⁴⁷ F. Happacher,¹⁷ K. Hara,⁵³ D. Hare,⁵⁰ M. Hare,⁵⁴ R. F. Harr,⁵⁷ K. Hatakeyama,⁶ C. Hays,⁴⁰ M. Heck,²⁴ J. Heinrich,⁴³ M. Herndon,⁵⁸ S. Hewamanage,⁶ D. Hidas,⁵⁰ A. Hocker,¹⁵ W. Hopkins,^{15,h} D. Horn,²⁴ S. Hou,¹ R. E. Hughes,³⁷ M. Hurwitz,¹¹ U. Husemann,⁵⁹ N. Hussain,³¹ M. Hussein,³³ J. Huston,³³ G. Introzzi,^{44a} M. Iori,^{49b,49a} A. Ivanov,^{7,p} E. James,¹⁵ D. Jang,¹⁰ B. Jayatilaka,¹⁴ E. J. Jeon,²⁵ M. K. Jha,^{6a} S. Jindariani,¹⁵ W. Johnson,⁷ M. Jones,⁴⁶ K. K. Joo,²⁵ S. Y. Jun,¹⁰ T. R. Junk,¹⁵ T. Kamon,⁵¹ P. E. Karchin,⁵⁷ A. Kasmi,⁶ Y. Kato,^{39,o} W. Ketchum,¹¹ J. Keung,⁴³ V. Khotilovich,⁵¹ B. Kilminster,¹⁵ D. H. Kim,²⁵ H. S. Kim,²⁵ H. W. Kim,²⁵ J. E. Kim,²⁵ M. J. Kim,¹⁷ S. B. Kim,²⁵ S. H. Kim,⁵³ Y. K. Kim,¹¹ N. Kimura,⁵⁶ M. Kirby,¹⁵ S. Klimenko,¹⁶ K. Kondo,⁵⁶ D. J. Kong,²⁵ J. Konigsberg,¹⁶ A. V. Kotwal,¹⁴ M. Kreps,²⁴ J. Kroll,⁴³ D. Krop,¹¹ N. Krumnack,^{6,m} M. Kruse,¹⁴ V. Krutelyov,^{51,e} T. Kuhr,²⁴ M. Kurata,⁵³ S. Kwang,¹¹ A. T. Laasanen,⁴⁶ S. Lami,^{44a} S. Lammel,¹⁵ M. Lancaster,²⁸ R. L. Lander,⁷ K. Lannon,^{37,w} A. Lath,⁵⁰ G. Latino,^{44b,44a} T. LeCompte,² E. Lee,⁵¹ H. S. Lee,¹¹ J. S. Lee,²⁵ S. W. Lee,^{51,y} S. Leo,^{44b,44a} S. Leone,^{44a} J. D. Lewis,¹⁵ A. Limosani,^{14,s} C.-J. Lin,²⁶ J. Linacre,⁴⁰ M. Lindgren,¹⁵ E. Lipeles,⁴³ A. Lister,¹⁸ D. O. Litvintsev,¹⁵ C. Liu,⁴⁵ Q. Liu,⁴⁶ T. Liu,¹⁵ S. Lockwitz,⁵⁹ N. S. Lockyer,⁴³ A. Loginov,⁵⁹ D. Lucchesi,^{41b,41a} J. Lueck,²⁴ P. Lujan,²⁶ P. Lukens,¹⁵ G. Lungu,⁴⁸ J. Lys,²⁶ R. Lysak,¹² R. Madrak,¹⁵ K. Maeshima,¹⁵ K. Makhoul,³⁰ P. Maksimovic,²³ S. Malik,⁴⁸ G. Manca,^{27,c} A. Manousakis-Katsikakis,³ F. Margaroli,⁴⁶ C. Marino,²⁴ M. Martínez,⁴ R. Martínez-Ballarín,²⁹ P. Mastrandrea,^{49a} M. Mathis,²³ M. E. Mattson,⁵⁷ P. Mazzanti,^{6a} K. S. McFarland,⁴⁷ P. McIntyre,⁵¹ R. McNulty,^{27,j} A. Mehta,²⁷ P. Mehtala,²¹ A. Menzione,^{44a} C. Mesropian,⁴⁸ T. Miao,¹⁵ D. Mietlicki,³² A. Mitra,¹ H. Miyake,⁵³ S. Moed,²⁰ N. Moggi,^{6a} M. N. Mondragon,^{15,l} C. S. Moon,²⁵ R. Moore,¹⁵ M. J. Morello,¹⁵ J. Morlock,²⁴ P. Movilla Fernandez,¹⁵ A. Mukherjee,¹⁵ Th. Muller,²⁴ P. Murat,¹⁵ M. Mussini,^{6b,6a} J. Nachtman,^{15,n} Y. Nagai,⁵³ J. Naganoma,⁵⁶ I. Nakano,³⁸ A. Napier,⁵⁴ J. Nett,⁵¹ C. Neu,⁵⁵ M. S. Neubauer,²² J. Nielsen,^{26,f} L. Nodulman,² O. Norniella,²² E. Nurse,²⁸ L. Oakes,⁴⁰ S. H. Oh,¹⁴ Y. D. Oh,²⁵ I. Oksuzian,⁵⁵ T. Okusawa,³⁹ R. Orava,²¹ L. Ortolan,⁴ S. Pagan Griso,^{41b,41a} C. Pagliarone,^{52a} E. Palencia,^{9,g} V. Papadimitriou,¹⁵ A. A. Paramonov,² J. Patrick,¹⁵ G. Pauletta,^{52b,52a} M. Paulini,¹⁰ C. Paus,³⁰ D. E. Pellett,⁷ A. Penzo,^{52a} T. J. Phillips,¹⁴ G. Piacentino,^{44a} E. Pianori,⁴³ J. Pilot,³⁷ K. Pitts,²² C. Plager,⁸ L. Pondrom,⁵⁸ K. Potamianos,⁴⁶ O. Poukhov,^{13,a} F. Prokoshin,^{13,z} A. Pronko,¹⁵ F. Ptohos,^{17,i} E. Pueschel,¹⁰ G. Punzi,^{44b,44a} J. Pursley,⁵⁸ A. Rahaman,⁴⁵ V. Ramakrishnan,⁵⁸ N. Ranjan,⁴⁶ I. Redondo,²⁹

P. Renton,⁴⁰ M. Rescigno,^{49a} F. Rimondi,^{6b,6a} L. Ristori,^{45,15} A. Robson,¹⁹ T. Rodrigo,⁹ T. Rodriguez,⁴³ E. Rogers,²² S. Rolli,⁵⁴ R. Roser,¹⁵ M. Rossi,^{52a} F. Rubbo,¹⁵ F. Ruffini,^{44c,44a} A. Ruiz,⁹ J. Russ,¹⁰ V. Rusu,¹⁵ A. Safonov,⁵¹ W. K. Sakumoto,⁴⁷ Y. Sakurai,⁵⁶ L. Santi,^{52b,52a} L. Sartori,^{44a} K. Sato,⁵³ V. Saveliev,^{42,v} A. Savoy-Navarro,⁴² P. Schlabach,¹⁵ A. Schmidt,²⁴ E. E. Schmidt,¹⁵ M. P. Schmidt,^{59,a} M. Schmitt,³⁶ T. Schwarz,⁷ L. Scodellaro,⁹ A. Scribano,^{44c,44a} F. Scuri,^{44a} A. Sedov,⁴⁶ S. Seidel,³⁵ Y. Seiya,³⁹ A. Semenov,¹³ F. Sforza,^{44b,44a} A. Sfyrla,²² S. Z. Shalhout,⁷ T. Shears,²⁷ P. F. Shepard,⁴⁵ M. Shimojima,^{53,u} S. Shiraishi,¹¹ M. Shochet,¹¹ I. Shreyber,³⁴ A. Simonenko,¹³ P. Sinervo,³¹ A. Sissakian,^{13,a} K. Sliwa,⁵⁴ J. R. Smith,⁷ F. D. Snider,¹⁵ A. Soha,¹⁵ S. Somalwar,⁵⁰ V. Sorin,⁴ P. Squillacioti,¹⁵ M. Stancari,¹⁵ M. Stanitzki,⁵⁹ R. St. Denis,¹⁹ B. Stelzer,³¹ O. Stelzer-Chilton,³¹ D. Stentz,³⁶ J. Strologas,³⁵ G. L. Strycker,³² Y. Sudo,⁵³ A. Sukhanov,¹⁶ I. Suslov,¹³ K. Takemasa,⁵³ Y. Takeuchi,⁵³ J. Tang,¹¹ M. Tecchio,³² P. K. Teng,¹ J. Thom,^{15,h} J. Thome,¹⁰ G. A. Thompson,²² E. Thomson,⁴³ P. Tito-Guzmán,²⁹ S. Tkaczyk,¹⁵ D. Toback,⁵¹ S. Tokar,¹² K. Tollefson,³³ T. Tomura,⁵³ D. Tonelli,¹⁵ S. Torre,¹⁷ D. Torretta,¹⁵ P. Totaro,^{41a} M. Trovato,^{44d,44a} Y. Tu,⁴³ F. Ukegawa,⁵³ S. Uozumi,²⁵ A. Varganov,³² F. Vázquez,^{16,1} G. Velev,¹⁵ C. Vellidis,³ M. Vidal,²⁹ I. Vila,⁹ R. Vilar,⁹ J. Vizán,⁹ M. Vogel,³⁵ G. Volpi,^{44b,44a} P. Wagner,⁴³ R. L. Wagner,¹⁵ T. Wakisaka,³⁹ R. Wallny,⁸ S. M. Wang,¹ A. Warburton,³¹ D. Waters,²⁸ M. Weinberger,⁵¹ W. C. Wester III,¹⁵ B. Whitehouse,⁵⁴ D. Whiteson,^{43,d} A. B. Wicklund,² E. Wicklund,¹⁵ S. Wilbur,¹¹ F. Wick,²⁴ H. H. Williams,⁴³ J. S. Wilson,³⁷ P. Wilson,¹⁵ B. L. Winer,³⁷ P. Wittich,^{15,h} S. Wolbers,¹⁵ H. Wolfe,³⁷ T. Wright,³² X. Wu,¹⁸ Z. Wu,⁶ K. Yamamoto,³⁹ J. Yamaoka,¹⁴ T. Yang,¹⁵ U. K. Yang,^{11,q} Y. C. Yang,²⁵ W.-M. Yao,²⁶ G. P. Yeh,¹⁵ K. Yi,^{15,n} J. Yoh,¹⁵ K. Yorita,⁵⁶ T. Yoshida,^{39,k} G. B. Yu,¹⁴ I. Yu,²⁵ S. S. Yu,¹⁵ J. C. Yun,¹⁵ A. Zanetti,^{52a} Y. Zeng,¹⁴ and S. Zucchelli^{6b,6a}

(CDF Collaboration)

¹*Institute of Physics, Academia Sinica, Taipei, Taiwan 11529, Republic of China*²*Argonne National Laboratory, Argonne, Illinois 60439, USA*³*University of Athens, 157 71 Athens, Greece*⁴*Institut de Física d'Altes Energies, ICREA, Universitat Autònoma de Barcelona, E-08193, Bellaterra (Barcelona), Spain*⁶*Baylor University, Waco, Texas 76798, USA*^{6a}*Istituto Nazionale di Fisica Nucleare Bologna, I-40127 Bologna, Italy*^{6b}*University of Bologna, I-40127 Bologna, Italy*⁷*University of California, Davis, Davis, California 95616, USA*⁸*University of California, Los Angeles, Los Angeles, California 90024, USA*⁹*Instituto de Física de Cantabria, CSIC-University of Cantabria, 39005 Santander, Spain*¹⁰*Carnegie Mellon University, Pittsburgh, Pennsylvania 15213, USA*¹¹*Enrico Fermi Institute, University of Chicago, Chicago, Illinois 60637, USA*¹²*Comenius University, 842 48 Bratislava, Slovakia; Institute of Experimental Physics, 040 01 Kosice, Slovakia*¹³*Joint Institute for Nuclear Research, RU-141980 Dubna, Russia*¹⁴*Duke University, Durham, North Carolina 27708, USA*¹⁵*Fermi National Accelerator Laboratory, Batavia, Illinois 60510, USA*¹⁶*University of Florida, Gainesville, Florida 32611, USA*¹⁷*Laboratori Nazionali di Frascati, Istituto Nazionale di Fisica Nucleare, I-00044 Frascati, Italy*¹⁸*University of Geneva, CH-1211 Geneva 4, Switzerland*¹⁹*Glasgow University, Glasgow G12 8QQ, United Kingdom*²⁰*Harvard University, Cambridge, Massachusetts 02138, USA*²¹*Division of High Energy Physics, Department of Physics, University of Helsinki and Helsinki Institute of Physics, FIN-00014, Helsinki, Finland*²²*University of Illinois, Urbana, Illinois 61801, USA*²³*The Johns Hopkins University, Baltimore, Maryland 21218, USA*²⁴*Institut für Experimentelle Kernphysik, Karlsruhe Institute of Technology, D-76131 Karlsruhe, Germany*²⁵*Center for High Energy Physics: Kyungpook National University, Daegu 702-701, Korea; Seoul National University, Seoul 151-742, Korea; Sungkyunkwan University, Suwon 440-746, Korea; Korea Institute of Science and Technology Information, Daejeon 305-806, Korea; Chonnam National University, Gwangju 500-757, Korea;**Chonbuk National University, Jeonju 561-756, Korea*²⁶*Ernest Orlando Lawrence Berkeley National Laboratory, Berkeley, California 94720, USA*²⁷*University of Liverpool, Liverpool L69 7ZE, United Kingdom*²⁸*University College London, London WC1E 6BT, United Kingdom*²⁹*Centro de Investigaciones Energéticas Medioambientales y Tecnológicas, E-28040 Madrid, Spain*³⁰*Massachusetts Institute of Technology, Cambridge, Massachusetts 02139, USA*

- ³¹*Institute of Particle Physics: McGill University, Montréal, Québec, Canada H3A 2T8; Simon Fraser University, Burnaby, British Columbia, Canada V5A 1S6; University of Toronto, Toronto, Ontario, Canada M5S 1A7; and TRIUMF, Vancouver, British Columbia, Canada V6T 2A3*
- ³²*University of Michigan, Ann Arbor, Michigan 48109, USA*
- ³³*Michigan State University, East Lansing, Michigan 48824, USA*
- ³⁴*Institution for Theoretical and Experimental Physics, ITEP, Moscow 117259, Russia*
- ³⁵*University of New Mexico, Albuquerque, New Mexico 87131, USA*
- ³⁶*Northwestern University, Evanston, Illinois 60208, USA*
- ³⁷*The Ohio State University, Columbus, Ohio 43210, USA*
- ³⁸*Okayama University, Okayama 700-8530, Japan*
- ³⁹*Osaka City University, Osaka 588, Japan*
- ⁴⁰*University of Oxford, Oxford OX1 3RH, United Kingdom*
- ^{41a}*Istituto Nazionale di Fisica Nucleare, Sezione di Padova-Trento, I-35131 Padova, Italy*
- ^{41b}*University of Padova, I-35131 Padova, Italy*
- ⁴²*LPNHE, Université Pierre et Marie Curie/IN2P3-CNRS, UMR7585, Paris, F-75252 France*
- ⁴³*University of Pennsylvania, Philadelphia, Pennsylvania 19104, USA*
- ^{44a}*Istituto Nazionale di Fisica Nucleare Pisa, I-56127 Pisa, Italy*
- ^{44b}*University of Pisa, I-56127 Pisa, Italy*
- ^{44c}*University of Siena, I-56127 Pisa, Italy*
- ^{44d}*Scuola Normale Superiore, I-56127 Pisa, Italy*
- ⁴⁵*University of Pittsburgh, Pittsburgh, Pennsylvania 15260, USA*
- ⁴⁶*Purdue University, West Lafayette, Indiana 47907, USA*
- ⁴⁷*University of Rochester, Rochester, New York 14627, USA*
- ⁴⁸*The Rockefeller University, New York, New York 10065, USA*
- ^{49a}*Istituto Nazionale di Fisica Nucleare, Sezione di Roma 1, I-00185 Roma, Italy*
- ^{49b}*Sapienza Università di Roma, I-00185 Roma, Italy*
- ⁵⁰*Rutgers University, Piscataway, New Jersey 08855, USA*
- ⁵¹*Texas A&M University, College Station, Texas 77843, USA*
- ^{52a}*Istituto Nazionale di Fisica Nucleare Trieste/Udine, I-34100 Trieste, Italy*
- ^{52b}*University of Trieste/Udine, I-33100 Udine, Italy*
- ⁵³*University of Tsukuba, Tsukuba, Ibaraki 305, Japan*
- ⁵⁴*Tufts University, Medford, Massachusetts 02155, USA*
- ⁵⁵*University of Virginia, Charlottesville, Virginia 22906, USA*
- ⁵⁶*Waseda University, Tokyo 169, Japan*
- ⁵⁷*Wayne State University, Detroit, Michigan 48201, USA*
- ⁵⁸*University of Wisconsin, Madison, Wisconsin 53706, USA*
- ⁵⁹*Yale University, New Haven, Connecticut 06520, USA*
- (Received 22 March 2011; published 27 July 2011)

A search for new dielectron-mass resonances using data recorded by the CDF II detector and corresponding to an integrated luminosity of 5.7 fb^{-1} is presented. No significant excess over the expected standard model prediction is observed. In this data set, an event with the highest dielectron mass ever observed ($960 \text{ GeV}/c^2$) was recorded. The results are interpreted in the Randall-Sundrum (RS) model. Combined with the 5.4 fb^{-1} diphoton analysis, the RS-graviton lower-mass limit for the coupling $k/\bar{M}_{\text{Pl}} = 0.1$ is $1058 \text{ GeV}/c^2$, making it the strongest limit to date.

DOI: 10.1103/PhysRevLett.107.051801

PACS numbers: 14.70.Kv, 11.25.Wx, 13.85.Qk, 13.85.Rm

Although extremely successful, the standard model (SM) of particles and fields is not sufficient for answering many open physics questions including the origin of dark matter, the incorporation of gravity, and the hierarchy between the weak and the Planck scales. Many extensions of the SM have been proposed, most of which predict the existence of new particles. The most direct way to discover a new unstable particle is through a mass resonance of its decay products. In this Letter we present a search for high-mass dielectron resonances.

At hadron colliders, the search for high-mass dilepton resonances has the advantage of very low hadronic

backgrounds and well-understood electroweak backgrounds. The search for dielectron resonances is additionally motivated by the event excess at a dielectron mass $M_{ee} = 240 \text{ GeV}/c^2$ reported by a CDF analysis [1] performed with an integrated luminosity of 2.5 fb^{-1} . Moreover, a recent CDF search [2] for Randall-Sundrum (RS) gravitons decaying to diphotons will benefit significantly from the addition of the dielectron decay channel. The RS model [3] solves the hierarchy problem by introducing an extra compact dimension accessible only to gravity. The phenomenology of this model leads to a small number of distinct Kaluza-Klein states (spin-2 gravitons

G) that couple to SM particles and can be individually detected as resonances of pairs of jets, leptons, photons, or gauge bosons. Other possible sources of dielectron resonances include the production of heavy spin-1 (e.g., Z' [4]) and spin-0 particles (e.g., Higgs boson [5] and supersymmetric particles [6]).

In this Letter we first present a model-independent search for dielectron resonances and we subsequently use the results to exclude part of the RS-graviton parameter space. The dielectron search is combined with the recent CDF diphoton RS-graviton search to set the strongest limits to date. Searches for dielectron resonances with RS-graviton interpretation have been previously published by the CDF [1] and D0 [7] Collaborations.

CDF II [8] is a multipurpose cylindrical detector with projective-tower calorimeter geometry and excellent lepton identification capability. It operates at Fermilab's Tevatron collider where protons and antiprotons collide with a center-of-mass energy of 1.96 TeV. In CDF's coordinate system the positive \hat{z} axis is defined by the proton beam direction and the positive \hat{y} axis by the vertical upward direction. The detector is approximately symmetric in the η and ϕ directions, where the pseudorapidity η is defined as $\eta = -\ln[\tan(\theta/2)]$, θ is the polar angle with respect to \hat{z} , and ϕ is the azimuthal angle.

The momentum p of charged particles is measured with a tracking system composed of an eight-layer silicon strip detector and a 96-layer drift chamber; both are located inside a solenoid providing a magnetic field of 1.4 T aligned along the beam axis. The tracking efficiency is nearly 100% in the central region ($|\eta| < 1$) and decreases in the forward region ($1 < |\eta| < 2.8$). Electromagnetic and hadronic calorimeters surround the solenoid and measure the energies of collision products up to $|\eta| = 3.6$. Gas Cherenkov counters measure the average number of inelastic $p\bar{p}$ collisions per bunch crossing and thereby determine the beam luminosity. A pipelined three-level trigger system [9] that combines hardware and software is used for filtering the collision data.

We perform an analysis of CDF dielectron data collected with a high transverse momentum ($p_T \equiv p \sin\theta > 18$ GeV/ c) central-electron trigger and corresponding to an integrated luminosity of 5.7 fb $^{-1}$. To ensure a uniform trigger response, we require the central electron to have $p_T > 20$ GeV/ c . A supplementary trigger, more efficient especially for electrons with $p_T > 70$ GeV/ c , is also used. The second electron can pass either through the central or forward detector region and it is required to have $p_T > 5$ GeV/ c . The tracking system provides the direction of the electrons, whereas the absolute value of their 3-momentum is determined from the energy deposited in the calorimeters. This energy deposition is required to geometrically match the track and the deposition's lateral shape must be consistent with that expected from electrons. The additional transverse calorimeter energy deposited in a cone of $\Delta R = \sqrt{(\Delta\phi)^2 + (\Delta\eta)^2} = 0.4$ around each

electron must be less than 10% of its transverse energy. The electrons are required to be separated by $\Delta R > 0.4$ and to have the z coordinate of their tracks at the origin within $|\Delta z| < 5$ cm. The average z position of the two tracks must be within 4 cm of an interaction vertex. Finally, each electron must have a track with an impact parameter less than 0.02 cm, if the track is reconstructed including information from the silicon detector, or less than 0.2 cm otherwise. The forward electrons can be linked to special silicon-only tracks in order to extend the reach in η beyond that of the drift chamber coverage. Because of the limitation in determining the charge of forward electrons, no opposite-charge requirement is imposed. After the above selection, we retain 240 224 dielectrons in the Z -boson resonance ($76 < M_{ee} < 106$ GeV/ c^2) and 801 dielectrons with $M_{ee} > 200$ GeV/ c^2 .

The main SM dielectron background to a high-mass dielectron signal is the Drell-Yan (DY) process $q\bar{q} \rightarrow Z/\gamma^* \rightarrow e^+e^-$. Secondary electroweak backgrounds come from diboson production ($WW, WZ, ZZ, W\gamma^*$) with subsequent electronic decays. The main hadronic background contributing to the dielectron candidate sample is the production of W + jets, where the W boson decays to an electron and a jet is misidentified as an electron ("fake" electron). Finally, $t\bar{t}$ events decaying to dielectrons are also considered.

The DY, diboson, and $t\bar{t}$ backgrounds are estimated with Monte Carlo (MC) simulation, using PYTHIA [10], running with the CTEQ5L [11] parton distribution functions, and the CDF GEANT-based [12] detector simulator. The MC events are normalized on an event-by-event basis using the theoretical next-to-leading-order (NLO) cross sections [13], event trigger efficiencies, electron identification scale factors, and data luminosity. Good agreement between SM expectation and CDF data in the Z resonance will validate our DY prediction. The diboson background estimation is validated in a trilepton $ee + e/\mu$ control region with $E_T > 15$ GeV [14], where the diboson contribution is significant. The $t\bar{t}$ dielectron background is validated in a control region with two or more hadronic jets, $H_T > 200$ GeV [15], and $E_T > 20$ GeV, where the top-quark pair production is the dominant process.

The hadronic (QCD) background is estimated using CDF data, by selecting events with an identified electron and applying to every well-reconstructed and fiducial jet a probability to be misidentified as an electron. The probability for a jet to fake an electron is determined from jet-rich CDF data [16]. The QCD background estimation is validated in the intermediate-mass ($20 < M_{ee} < 76$ GeV/ c^2) control region, as well as in the trilepton ($76 < M_{ee} < 106$ GeV/ c^2) and high-mass $t\bar{t}$ control regions described above.

The main sources of systematic uncertainty on the MC-estimated backgrounds [17] are the theoretical cross sections (an 8% effect on the event yields), the luminosity

(6%), the lepton-ID efficiency (2%), the parton distribution functions (2%), and the trigger efficiency (0.5%). The total MC systematic uncertainty on the expected event yield is $\sim 10\%$. The respective QCD-background systematic uncertainty is $\sim 50\%$, which comes from the variation in the measurement of the fake probabilities using different jet-rich CDF data sets triggered with varied jet-energy thresholds. Since the SM background is very low in the high dielectron-mass region of interest, the results are not overly sensitive to the systematic uncertainties.

Figure 1(a) shows the M_{ee} spectrum for SM expectation and CDF data. We observe good agreement in the Z -boson resonance region, which validates our efficiencies, scale factors, data luminosity, and theoretical cross sections. We observe a long mass tail coming mainly from the DY process. Figure 1(b) shows the M_{ee} spectrum between 200 and 600 GeV/c^2 ; above 200 GeV/c^2 , we expect 793 ± 96 events and observe 801. The previously observed excess in the 225–250 GeV/c^2 region [1] has been reduced to a $<1\text{-}\sigma$ effect, in this larger data set. We observe

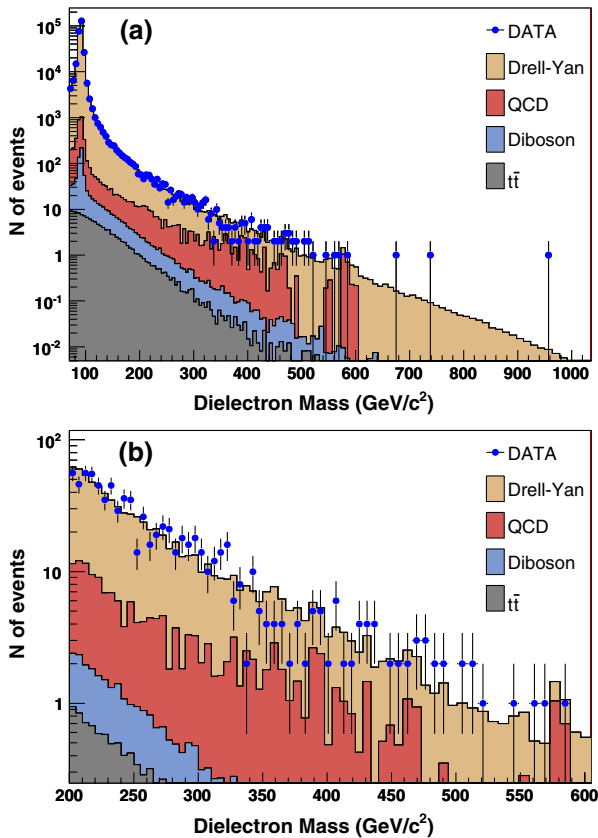


FIG. 1 (color online). (a) The dielectron-mass distribution for the SM background (stacked histograms of DY, QCD, diboson, and $t\bar{t}$) and the CDF data. The QCD background is derived from CDF data. The electroweak backgrounds are estimated using MC normalized to the data luminosity times theoretical cross sections, without fitting to any part of the dielectron data distribution. (b) The dielectron-mass distribution between 200 and 600 GeV/c^2 .

an exceptional $M_{ee} = 960 \text{ GeV}/c^2$ candidate event, the highest-mass dielectron event ever observed. Calorimeter resolution induces an uncertainty on the dielectron mass of 16 GeV/c^2 for this event. The two electrons have transverse momenta of 482 and 468 GeV/c ; they originate from the same primary vertex and are oppositely charged. The event is characterized by very low hadronic activity (no jets are reconstructed) and by a low missing transverse energy of 17 GeV —separated by 23° in ϕ from the 468 GeV/c electron—coming most probably from the resolution of the calorimeter.

In order to assess the agreement between SM and observation, for every mass bin i we define a p value as the probability to observe at least N_{data}^i events, when N_{SM}^i events are expected. We determine this probability by generating pseudoexperiments and counting the number of times when $N_{\text{pseudo}}^i \geq N_{\text{data}}^i$. Here N_{pseudo}^i follows a Poisson distribution convoluted with a Gaussian of mean equal to N_{SM}^i and standard deviation equal to the SM systematic uncertainty for the i th bin. Figure 2 shows the p value as a function of the M_{ee} . The band defines the $1\text{-}\sigma$ expected range of the minimum p value that could be observed in any mass bin. This range is calculated from the probability distribution of minimum p values determined with the use of pseudoexperiments. The probability to observe a SM event with $M_{ee} \geq 960 \text{ GeV}/c^2$ is 4%. Above 600 GeV/c^2 , we expect 3.6 ± 0.4 events and observe three. The second most significant excess of events is observed at $\sim 320 \text{ GeV}/c^2$, as shown in Fig. 2.

The measured M_{ee} spectrum can be used to set a limit on RS-graviton production. Here we parametrize the RS model using the mass of the lightest RS graviton (m_1) and the dimensionless parameter $\sqrt{8\pi}k/M_{\text{Pl}} \equiv k/\bar{M}_{\text{Pl}}$, where k is the curvature scale of the extra dimension and M_{Pl} is the Planck mass. RS-graviton signal MC-simulated samples are generated using PYTHIA and values of m_1 from 200 to 1100 GeV/c^2 . The signal-MC events are normalized in the same manner as the background-MC

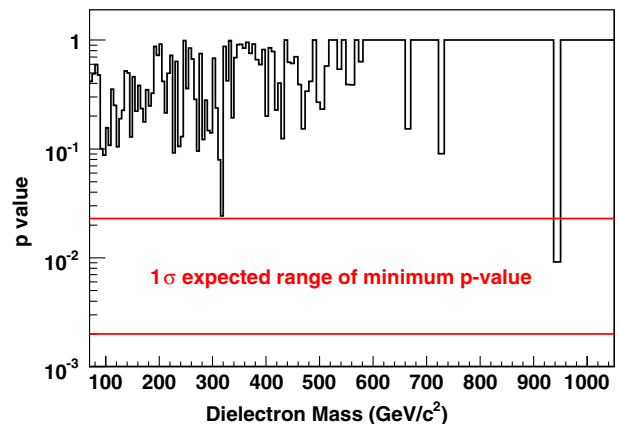


FIG. 2 (color online). The p value as a function of the dielectron mass. The $1\text{-}\sigma$ range of expected minimum p value seen at any bin is shown.

events. The leading-order PYTHIA cross section is multiplied by a scale (“ K factor”) to correct for next-to-leading-order effects. The CDF acceptance for the dielectron RS-graviton signal, determined using the MC signal samples, is $\sim 27\%$. The acceptance is approximately independent of the RS-graviton mass due to the inclusion of forward electrons, as lower-mass gravitons ($m_1 < 700 \text{ GeV}/c^2$) would decay to at least one forward lepton more often than higher-mass gravitons. The RS graviton decays to two jets (branching ratio $\text{BR} = 70\%$), or two charged leptons ($\text{BR} = 6\%$), or two neutrinos ($\text{BR} = 6\%$), or two photons ($\text{BR} = 4\%$), or two weak bosons ($\text{BR} = 14\%$). For graviton masses above $200 \text{ GeV}/c^2$, these branching ratios are graviton-mass independent. Given the considerable dijet background in a hadron-collider environment, and the low leptonic branching fraction of the weak bosons, the prompt dilepton and diphoton final states offer the greatest sensitivity. The inclusion of dielectrons in the diphoton RS search [2] results in a 50% increase in the rate of potentially produced signal. Here we present the cross section and mass limits for the dielectron channel alone and for the combined dielectron and diphoton channels.

Figure 3(a) shows the 95% confidence level (C.L.) cross section [$\sigma \times \text{BR}(G \rightarrow ee)$] upper limit as a function of the lightest RS-graviton mass m_1 along with five theoretical cross-section curves for $k/\bar{M}_{\text{Pl}} = 0.01$ to 0.1 , a theoretically interesting range that would provide a solution for the hierarchy problem. The limits are set using a frequentist method that compares the background-only with the signal+background hypotheses, taking into account correlated background systematic uncertainties [2,18]. The intersection of the cross-section exclusion limit with the theoretical cross-section curves gives the 95% C.L. lower limit on m_1 for the respective coupling. For $k/\bar{M}_{\text{Pl}} = 0.1$, the dielectron-only m_1 lower limit is $914 \text{ GeV}/c^2$, if we use proper mass-dependent RS-graviton K factors [19,20], and $935 \text{ GeV}/c^2$ assuming a fixed K factor of 1.54 [7], for comparison with previous results [1,7]. For $m_1 > 700 \text{ GeV}/c^2$, the dielectron-only analysis excludes cross sections greater than 2 fb at the 95% C.L. Figure 3(b) shows the 95% C.L. cross section [$\sigma \times \text{BR}(G \rightarrow ee/\gamma\gamma)$] upper limit from the combination of the dielectron and diphoton analyses. The two analyses are combined as independent channels bound by a common production cross section and some correlated systematic uncertainties [18]. For $k/\bar{M}_{\text{Pl}} = 0.1$, the combined m_1 lower limit is $1058 \text{ GeV}/c^2$, if we use proper mass-dependent RS-graviton K factors, and $1092 \text{ GeV}/c^2$ assuming a fixed K factor of 1.54. For $m_1 > 700 \text{ GeV}/c^2$, the combined $ee/\gamma\gamma$ analysis excludes cross sections greater than 0.9 fb at the 95% C.L.

Figure 4 shows the exclusions in the k/\bar{M}_{Pl} vs m_1 parameter space for the dielectron analysis, the diphoton analysis and their combination. For $k/\bar{M}_{\text{Pl}} = 0.1$, the

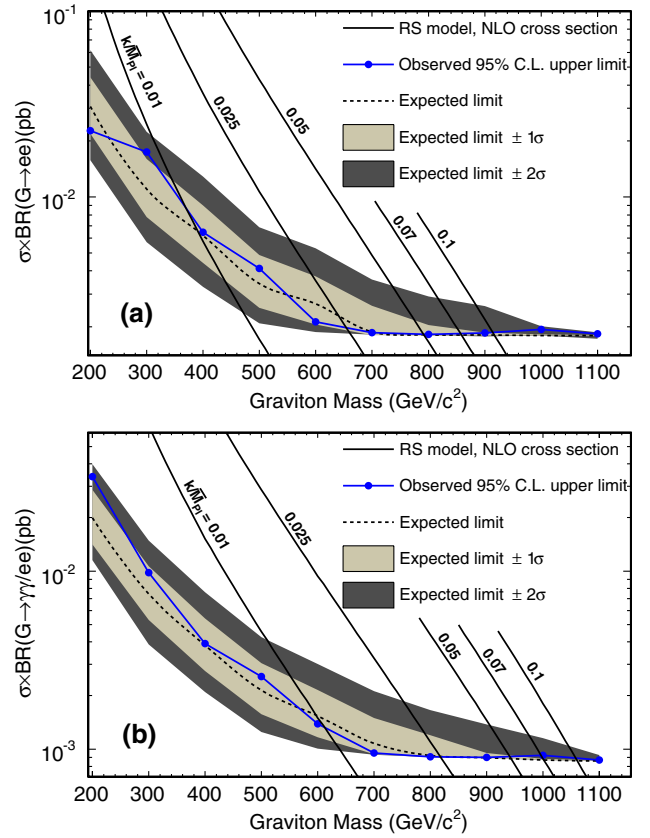


FIG. 3 (color online). (a) The 95% C.L. upper limit on the lightest RS-graviton production cross section from the dielectron analysis, as a function of the graviton’s mass. (b) The respective cross section and mass limits for the combination of the dielectron and diphoton analyses.

inclusion of electrons improves the previous CDF RS-graviton limit [2] by $\sim 95 \text{ GeV}/c^2$ and surpasses the previous published [7] best limit by $\sim 40 \text{ GeV}/c^2$. Table I summarizes the combined $ee/\gamma\gamma$ RS-graviton lower-mass limits for different values of k/\bar{M}_{Pl} .

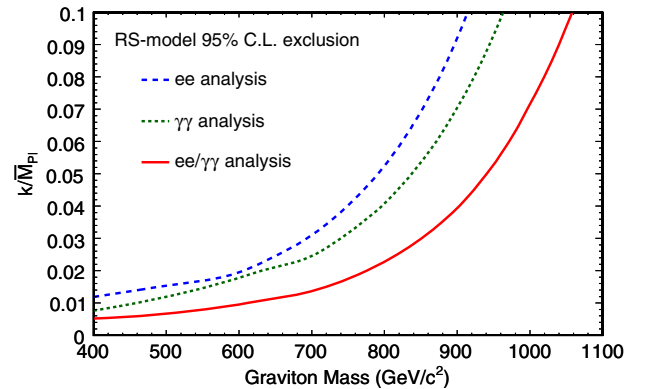


FIG. 4 (color online). The area excluded in the k/\bar{M}_{Pl} vs m_1 RS-model parameter space by the 5.7 fb^{-1} dielectron analysis (area above long-dashed line), the 5.4 fb^{-1} diphoton analysis (area above short-dashed line), and their combination (area above solid line).

TABLE I. The 95% C.L. RS-graviton lower mass limits from the combined $ee/\gamma\gamma$ analysis, for five values of k/\bar{M}_{Pl} .

k/\bar{M}_{Pl}	Mass limit (GeV/ c^2)
0.01	612
0.025	818
0.05	941
0.07	997
0.1	1058

In summary, we present a search for high-mass dielectron resonances using CDF data corresponding to an integrated luminosity of 5.7 fb^{-1} . We do not observe any significant discrepancies from the expected SM prediction, while we detect the highest-mass dielectron event ever observed, at $960 \text{ GeV}/c^2$. We use the dielectron-mass spectrum to set 95% C.L. limits on the RS-graviton production, for several values of the k/\bar{M}_{Pl} parameter. The graviton-mass lower limit from the combined dielectron and diphoton analyses and for $k/\bar{M}_{\text{Pl}} = 0.1$ is 1058 or $1092 \text{ GeV}/c^2$, depending on the assumption on the NLO cross sections, making this result the most stringent to date.

We thank M. C. Kumar, P. Mathews, and V. Ravindran for the calculation of the mass-dependent RS-graviton K factors. We also thank the Fermilab staff and the technical staffs of the participating institutions for their vital contributions. This work was supported by the U.S. Department of Energy and National Science Foundation; the Italian Istituto Nazionale di Fisica Nucleare; the Ministry of Education, Culture, Sports, Science and Technology of Japan; the Natural Sciences and Engineering Research Council of Canada; the National Science Council of the Republic of China; the Swiss National Science Foundation; the A. P. Sloan Foundation; the Bundesministerium für Bildung und Forschung, Germany; the Korean World Class University Program, the National Research Foundation of Korea; the Science and Technology Facilities Council and the Royal Society, U.K.; the Institut National de Physique Nucleaire et Physique des Particules/CNRS; the Russian Foundation for Basic Research; the Ministerio de Ciencia e Innovación, and Programa Consolider-Ingenio 2010, Spain; the Slovak R&D Agency; the Academy of Finland; and the Australian Research Council (ARC).

^aDeceased.^bVisitor from University of Massachusetts Amherst, Amherst, MA 01003, USA.^cVisitor from Istituto Nazionale di Fisica Nucleare, Sezione di Cagliari, 09042 Monserrato (Cagliari), Italy.^dVisitor from University of California Irvine, Irvine, CA 92697, USA.^eVisitor from University of California Santa Barbara, Santa Barbara, CA 93106, USA.^fUniversity of California Santa Cruz, Santa Cruz, CA 95064, USA.^gVisitor from CERN, CH-1211 Geneva, Switzerland.^hVisitor from Cornell University, Ithaca, NY 14853, USA.ⁱVisitor from University of Cyprus, Nicosia CY-1678, Cyprus.^jVisitor from University College Dublin, Dublin 4, Ireland.^kVisitor from University of Fukui, Fukui City, Fukui Prefecture, Japan 910-0017.^lVisitor from Universidad Iberoamericana, Mexico D.F., Mexico.^mVisitor from Iowa State University, Ames, IA 50011, USA.ⁿVisitor from University of Iowa, Iowa City, IA 52242, USA.^oVisitor from Kinki University, Higashi-Osaka City, Japan 577-8502.^pVisitor from Kansas State University, Manhattan, KS 66506, USA.^qVisitor from University of Manchester, Manchester M13 9PL, U.K.^rVisitor from Queen Mary, University of London, London, E1 4NS, U.K.^sVisitor from University of Melbourne, Victoria 3010, Australia.^tVisitor from Muons, Inc., Batavia, IL 60510, USA.^uVisitor from Nagasaki Institute of Applied Science, Nagasaki, Japan.^vVisitor from National Research Nuclear University, Moscow, Russia.^wVisitor from University of Notre Dame, Notre Dame, IN 46556, USA.^xVisitor from Universidad de Oviedo, E-33007 Oviedo, Spain.^yVisitor from Texas Tech University, Lubbock, TX 79609, USA.^zVisitor from Universidad Tecnica Federico Santa Maria, 110v Valparaiso, Chile.^{aa}Visitor from Yarmouk University, Irbid 211-63, Jordan.^{bb}On leave from J. Stefan Institute, Ljubljana, Slovenia.

- [1] T. Aaltonen *et al.* (CDF Collaboration), *Phys. Rev. Lett.* **102**, 031801 (2009).
- [2] T. Aaltonen *et al.* (CDF Collaboration), *Phys. Rev. D* **83**, 011102(R) (2011).
- [3] L. Randall and R. Sundrum, *Phys. Rev. Lett.* **83**, 3370 (1999).
- [4] P. Langacker, *Rev. Mod. Phys.* **81**, 1199 (2009).
- [5] P. W. Higgs, *Phys. Rev. Lett.* **13**, 508 (1964).
- [6] H. Baer and X. Tata, *Weak Scale Supersymmetry* (Cambridge University Press, Cambridge, U.K., 2006).
- [7] V. M. Abazov *et al.* (D0 Collaboration), *Phys. Rev. Lett.* **104**, 241802 (2010).
- [8] D. Acosta *et al.* (CDF Collaboration), *Phys. Rev. D* **71**, 032001 (2005).
- [9] R. Downing *et al.*, *Nucl. Instrum. Methods Phys. Res., Sect. A* **570**, 36 (2007).
- [10] T. Sjöstrand, L. Lönnblad, and S. Mrenna, *arXiv:hep-ph/0108264*.
- [11] H. Lai *et al.* (CTEQ Collaboration), *Eur. Phys. J. C* **12**, 375 (2000).

- [12] R. Brun, R. Hagelberg, M. Hansroul, and J. Lasalle, CERN Report No. CERN-DD-78-2-REV, 1978.
- [13] A. D. Martin, W. J. Stirling, R. S. Thorne, and G. Watt, *Eur. Phys. J. C* **63**, 189 (2009); J. M. Campbell and R. K. Ellis, *Phys. Rev. D* **60**, 113006 (1999); N. Kidonakis and R. Vogt, *Phys. Rev. D* **78**, 074005 (2008).
- [14] The missing transverse energy vector E_T is defined as $-(\sum_i \vec{E}_i)_T$, where \vec{E}_i has magnitude equal to the energy deposited in the i th calorimeter tower and direction perpendicular to the beam axis and pointing to that calorimeter tower. The E_T is corrected for the presence of muons, because they do not deposit their energy in the calorimeters.
- [15] H_T is defined as the scalar sum of the transverse momenta of jets, leptons and E_T .
- [16] M. Vogel, Ph.D. thesis, University of New Mexico, 2011 (to be published).
- [17] T. Aaltonen *et al.* (CDF Collaboration), *Phys. Rev. D* **79**, 052004 (2009).
- [18] T. Junk, *Nucl. Instrum. Methods Phys. Res., Sect. A* **434**, 435 (1999).
- [19] P. Mathews, V. Ravindran, and K. Sridhar, *J. High Energy Phys.* **10** (2005) 031; (private communication).
- [20] M. C. Kumar, P. Mathews, and V. Ravindran, *Eur. Phys. J. C* **49**, 599 (2006).